



Power-based modelling of renewable variability in dispatch models with clustered time periods

Elis Nycander^{a, *}, Germán Morales-España^b, Lennart Söder^a

^a KTH Royal Institute of Technology, Stockholm, Sweden

^b TNO Energy Transition, Amsterdam, the Netherlands

ARTICLE INFO

Article history:

Received 5 October 2021

Received in revised form

11 December 2021

Accepted 24 December 2021

Available online 30 December 2021

Keywords:

Economic dispatch

Power system planning

Hydro power planning

Renewable generation

Power-based model

ABSTRACT

The planning of future power systems with high shares of renewable generation requires modelling large and complex systems over long time periods, resulting in models which are computationally heavy to solve. For this reason methods that can be used to decrease the size of power system dispatch models are needed. A common method in large scale planning models is to decrease the model size by increasing the size of the time steps. However, using larger time steps makes the representation of variability of renewable generation and load less accurate, which can affect the results from the model. In this paper, we investigate the possibility to use a power-based version of an economic dispatch model to decrease the model time resolution while getting results which are close to the original high-resolution model. We implement both power-based and the conventional, energy-based, versions of a dispatch model with different time resolutions, and show that the power-based model has better agreement with the high-resolution model, especially as the model time step increases. For example, using the power-based model gives more accurate results for wind power curtailment in a high-renewable scenario.

© 2022 The Authors. Published by Elsevier Ltd. This is an open access article under the CC BY license (<http://creativecommons.org/licenses/by/4.0/>).

1. Introduction

Power systems world wide are undergoing big changes, as variable renewable energy (VRE) sources are replacing conventional fossil-based thermal generation. One of the main challenges of operating power systems that rely on VRE production for a large share of the generation is its variability. Due to its weather dependence, VRE production is variable both on short and long time scales. Wind power production from individual wind farms is highly variable on an hourly and intra-hourly basis, but the short-term variability is decreased when aggregating a large number of wind farms [1,2]. Nevertheless, a country like Sweden can see hourly ramp events close to 30% of installed wind power capacity [3]. There are also low-wind periods: In Germany there is on average one period per year when the wind capacity factor drops below 10% for around five consecutive days [4]. Wind power is also variable on an annual basis giving, e.g., annual variations of $\pm 7.5\%$ for a 32 year period in the U.S. [5], but shows considerably less variability than yearly hydro power production. Solar power has

more short-term variability than wind power, but usually a higher correlation with demand [6].

Planning for future power systems that can deal with the impact of VRE variability requires large-scale power system models that are run for extended periods of time (months to years), to simulate the expansion and operation of the power system. Notably, generation expansion planning (GEP) models [7] are used to optimize expansion of both generation and transmission capacity. Many studies are also focused on investigating the potential of specific renewable technologies to meet future projected power demands. For example [8], investigated the potential for wind power integration in China, using modelled wind speed data to determine wind power production under different scenarios for wind power capacity expansion, and [9] used a wind power production and dispatch model to analyse wind power curtailments under different penetration levels. Several other studies also looked at wind power curtailments, such as [10] which analysed wind curtailments in a future Nordic power system, and [11] which analysed the need for wind power curtailments in Ireland. Other studies have focused on the effects of renewable generation on electricity prices [12] and on the effect of VRE forecasts for large-scale hydro-thermal scheduling problems [13]. Another important research area is power system reliability, and how it is effected by increased VRE production.

* Corresponding author.

E-mail addresses: elisn@kth.se (E. Nycander), german.morales@tno.nl (G. Morales-España), lsod@kth.se (L. Söder).

Nomenclature			
Sets			
\mathcal{A}	price areas, indexed a	\overline{W}_{at}^e	available wind generation in area a for time step $t \in \mathcal{T}$, in energy [GWh]
$\mathcal{A}^H \subset \mathcal{A}$	price areas with hydro generation	\overline{W}_{at}^p	available wind generation in area a for time $t \in \mathcal{I}$, in power [GW]
\mathcal{G}	nuclear and thermal generators, indexed g	\overline{X}_{ct}^e	maximum limit for transfer on connection $c \in \mathcal{C}^l$ for time step $t \in \mathcal{T}$, in energy [GWh]
$\mathcal{G}^T \subset \mathcal{G}$	thermal generators	\overline{X}_{ct}^p	maximum limit for transfer on connection $c \in \mathcal{C}^l$ for time $t \in \mathcal{I}$, in power [GW]
\mathcal{C}^l	internal one-directional connections ($a_1 \rightarrow a_2$), indexed c	Z_{ct}^e	transfer on connection $c \in \mathcal{C}^E$ for time step $t \in \mathcal{T}$, in energy [GWh]
\mathcal{C}^E	external connections ($a \rightarrow \text{ext}$) with fixed transfer, indexed c	Z_{ct}^p	transfer on connection $c \in \mathcal{C}^E$ for time $t \in \mathcal{I}$, in power [GW]
$\mathcal{C}^{DC} \subset \mathcal{C}^l$	internal HVDC connections		
\mathcal{T}	time steps, indexed $t = 1, \dots, T$	Variables	
\mathcal{I}	instantaneous time marking beginning of each time step, indexed $t = 1, \dots, T + 1$	d_{at}^e	demand reduction in area a for time step $t \in \mathcal{T}$, in energy [GWh]
Parameters		d_{at}^p	demand reduction in area a for time $t \in \mathcal{I}$, in power [GW]
Δ	number of hours in model time step [h]	p_{gt}^e	production from generator $g \in \mathcal{G}$ for time step $t \in \mathcal{T}$, in energy [GWh]
η	loss fraction for internal connections	p_{gt}^p	production from generator $g \in \mathcal{G}$ for time $t \in \mathcal{I}$, in power [GW]
μ	ramp penalization factor for power-based model	pv_{at}^e	dispatched solar generation in area a for time step $t \in \mathcal{T}$, in energy [GWh]
C_{gt}	cost function for generator $g \in \mathcal{G}$ and time $t \in \mathcal{T}$ [EUR]	pv_{at}^p	dispatched solar generation in area a for time $t \in \mathcal{I}$, in power [GW]
C^W	cost of wind generation, 1000 EUR/GWh	r_{at}	reservoir content in area a at time $t \in \mathcal{I}$ [GWh]
\overline{D}_{at}^e	nominal demand in area a for time step $t \in \mathcal{T}$, in energy [GWh]	res_{at}^e	reservoir hydro production in area a for time step $t \in \mathcal{T}$, in energy [GWh]
\overline{D}_{at}^p	nominal demand in area a for time $t \in \mathcal{I}$, in power [GW]	res_{at}^p	reservoir hydro production in area a for time $t \in \mathcal{I}$, in power [GW]
$\underline{H}_a, \overline{H}_a$	min/max hydro generation levels for area a [GW]	ror_{at}^e	run of river hydro production in area a for time step $t \in \mathcal{T}$, in energy [GWh]
I_{at}	total reservoir inflow in area a for time t [GWh]	ror_{at}^p	run of river hydro production in area a for time $t \in \mathcal{I}$, in power [GW]
$\underline{P}_g, \overline{P}_g$	min/max generation levels for generator $g \in \mathcal{G}$ [GW]	s_{at}	spillage from reservoir in area a for time step $t \in \mathcal{T}$ [GWh]
\overline{PV}_{at}^e	available solar generation in area a for time step $t \in \mathcal{T}$, in energy [GWh]	w_{at}^e	dispatched wind generation in area a for time step $t \in \mathcal{T}$, in energy [GWh]
\overline{PV}_{at}^p	available solar generation in area a for time $t \in \mathcal{I}$, in power [GW]	w_{at}^p	dispatched wind generation in area a for time $t \in \mathcal{I}$, in power [GW]
\overline{R}_a	maximum reservoir level for area a [GWh]	x_{ct}^e	transfer for connection $c \in \mathcal{C}^l$ for time step $t \in \mathcal{T}$, in energy [GWh]
$R_a^{\text{end}/\text{ini}}$	final/initial reservoir level for area a [GWh]	x_{ct}^p	transfer for connection $c \in \mathcal{C}^l$ for time $t \in \mathcal{I}$, in power [GW]
RU_g, RD_g	max/min ramp rates for generator $g \in \mathcal{G}$ [GW/h]	$\delta_{gt}^{+/-}$	variables to penalize ramp excursions for generator $g \in \mathcal{G}^T$ for time $t \in \mathcal{T}$
RU_a^H, RD_a^H	max/min ramp rates for hydro generation in area a [GW/h]		
RU^{DC}, RD^{DC}	max/min ramp rates for HVDC connections [GW/h]		
\overline{ROR}_{at}^e	run of river inflow in area a for time step $t \in \mathcal{T}$, in energy [GWh]		
\overline{ROR}_{at}^p	run of river inflow in area a for time $t \in \mathcal{I}$, in power [GW]		
$VOLL$	value of lost load, $3 \cdot 10^6$ EUR/GWh		

Studies of power system reliability require computationally demanding simulations using techniques such as sequential Monte Carlo simulation [14,15].

Although there are many differences between these studies in terms of purpose and scope, they all have in common that they rely on a dispatch model for the power system, to obtain the optimal power system dispatch under different conditions. It is then desirable to have a dispatch model that imposes a low computational burden. Firstly, these dispatch models are often solved for large systems and long time spans, making them computationally challenging. In GEP models, this problem is commonly handled by limiting the time span for which the dispatch model is solved. For

example [16], models the power system dispatch for 576 h out of a 20 year planning horizon [17], models the dispatch for 7 days during a year, and the MARKAL energy systems model [18] represents the electricity dispatch in each year by 6 time periods. Decreasing the number of time steps for which the dispatch is simulated can affect the results of the model significantly, but is usually unavoidable to make the model size tractable. For example, in Ref. [19] it was found that increasing the number of simulated periods by a factor of 7 increased the system cost by 9.5% for a European-scale energy systems investment planning model. The more complexity is added to the model in other aspects, such as sector coupling or increasing the system size, the greater will be the

need to reduce the complexity imposed by the dispatch model. An example of this is the study of the Chinese power system in Ref. [8], which used a heuristic technique based on different production categories to calculate the dispatch in different periods, since using a proper dispatch model would be computationally challenging.

Secondly, apart from being solved for large systems, it is often needed to solve these dispatch models for many scenarios, e.g., for assessment of generation adequacy and operational security. A prominent example is the ENTSO-E Mid Term Adequacy Assessment (MAF), which is based on Monte-Carlo simulation of different weather years and outages. The adequacy estimates are then obtained using repeated simulation of the dispatch model to compute the unserved load [20].

Finally, properly accounting for uncertainty in power systems with significant amounts of VRE production requires stochastic optimization methods which also increases the computational complexity of the models and hence increases the need for small but realistic dispatch models. For example, in Ref. [13], which looked at the impact of using extended weather forecasts for operation scheduling in the Nordic power system, it took at least 27 h to solve the stochastic model even with 6 h time steps.

As the power system moves towards increasing penetration of renewables, stochastic methods which increase the computational complexity will be needed for operation simulation and GEP models. For these reasons, methods that can be used to decrease the size and solution time of dispatch models while maintaining sufficient modelling accuracy are needed. In this paper, we investigate the possibility to speed up a dispatch model by converting it into a power-based model. Conventional dispatch models describe the production profiles of units as discrete energy blocks, as further explained in Section 2. This has the downside of not capturing the continuous trajectories of demand and variable renewable production, and also not correctly representing unit ramps. For this reason, a power-based unit commitment (UC) formulation has been proposed in Refs. [21,22] and shown to significantly increase the performance of UC formulations, in different settings such as when dealing with wind power uncertainty [23] and when considering N-1 security constraints [24]. In this paper we convert an existing dispatch model for the Nordic power system [10] into a power-based version, and evaluate the benefits of using the power-based model compared to the energy-based model, while decreasing the time resolution in the model in order to lower solution times.

A comparison of the power-based and energy-based UC formulations with different time durations was carried out in Ref. [25], but with increased time resolution, i.e., using time steps shorter than 1 h, to investigate the effect of using shorter market trading intervals. It was found that using power-based scheduling as opposed to energy-based scheduling can reduce total operation costs by several percentage points, and that the power-based formulation leads to better scheduling decisions even when the time resolution is decreased to 5 min. In this study, we look at using decreased time resolution in order to decrease the model size, thus providing the first comparison of the power-based and energy-based formulations using clustered time periods. Additionally, the novelty of the study lies in investigating the impact of using the power-based formulation for a dispatch model meant for medium to long-term power operation simulation and wind integration studies, as opposed to a UC formulation directed mainly at short-term scheduling. Finally, our model includes a significant amount of hydro power, and is thus the first case where the power-based formulation is applied to the hydro-thermal scheduling problem.

We implement both power-based and energy-based versions of the dispatch model with different time resolutions ranging from 1 h to 6 h. In order to compare the models a 15-min time resolution benchmark model is used. To facilitate a fair comparison the time

series used in the low resolution models are constructed from the 15-min time series. For the power-based model, we suggest a method for fitting the power profiles which results in a quadratic programme and thus guarantees finding the global optimum.

The power-based and energy-based models are compared in terms of how well they reproduce the results of the 15-min benchmark model, when simulating the Nordic power system over one year. It is shown that the power-based model gives better results both when looking at a case with curtailment, due to increased VRE production, and a case with load shedding due to decreased conventional generation capacity. This means that the power-based version of the dispatch model can be useful for applications where model size is critical, since a low resolution version of the power-based model will be more accurate compared to an energy-based version. For example, the power-based model with decreased time resolution can be used for renewable integration studies where stochastic modelling of uncertainty of renewable generation is required, in order to decrease the model size while giving more accurate results for load shedding and VRE curtailment.

The remainder of the paper is structured as follows. First Section 2 explains the concept of power-based modelling and compares it to the traditional energy-based modelling. Next, Section 3 gives the formulation of the models and describes the method used to obtain the time series inputs to the models. Section 4 then compares the formulations using two case studies, and Section 5 shows sensitivity analysis of the results with respect to different model settings. Finally, Section 6 concludes.

2. Power-based and energy-based modelling

In traditional energy system models, continuous quantities such as electricity demand and generation are approximated to discrete time periods using staircase functions by modelling the average energy quantity during a time step, as illustrated in Fig. 1. This type of modelling has the drawback of not accurately capturing the ramp rates of continuous quantities [26], and a power-based formulation was proposed in Refs. [22,27] to overcome the drawbacks of traditional energy-based UC formulations.

Fig. 1 shows an example illustrating the benefits of the power-based formulation for modelling ramp rates. We assume that a unit has min/max generation levels of 100 MW and 500 MW, respectively, and a maximum ramp rate of 200 MW/h. Notice that this unit may represent an individual power plant or an aggregation of several smaller power plants, as is common in large scale dispatch

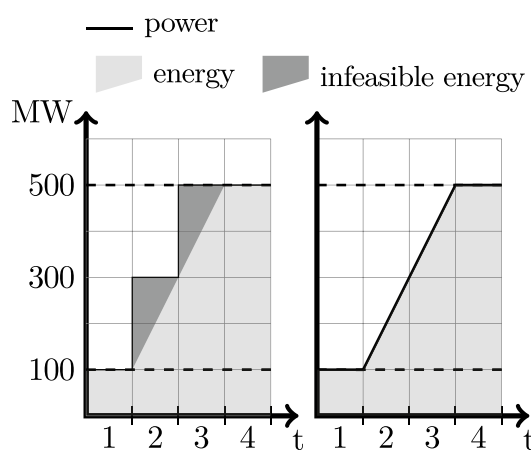


Fig. 1. Representation of ramps using energy-based (left) and power-based (right) formulation.

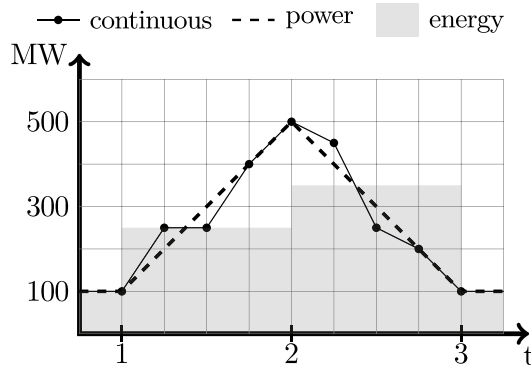


Fig. 2. Representation of wind variability using energy-based and power-based formulation. The x-axis labels mark the beginning of each model time period.

models such as [10]. It is assumed that the energy production of the unit during hour 1 is 100 MWh, which means that it must operate at its minimum output level for the whole hour. Then, assuming the unit must increase its output to meet demand, Fig. 1 shows how the production profile can look with energy-based and power based scheduling. Using the energy-based formulation and imposing the ramp rate requirement of 200 MW/h on energy quantities, the unit can ramp to 300 MWh during hour 2 and 500 MWh during hour 3. However, since the unit starts hour 2 at 100 MW, the maximum power output at the end of hour 2 is 300 MW, and the corresponding maximum energy output only 200 MWh, and similarly for hour 3. Thus, the energy schedule resulting from the energy-based formulation is in fact infeasible for the unit to provide, as shown by the dark shaded area in Fig. 1. On the other hand, using the power-based formulation correctly represents the unit’s ramp rate and produces a feasible power and energy schedule.

Apart from better modelling the ramp rates of units, the power-based approach can also better represent variability of VRE production and load. This is illustrated in Fig. 2, which shows an example of a wind production profile during two model time steps. The original wind profile has higher time resolution than the time step of the model and is considered as the continuous wind profile, though the resolution in this example is only 4 times the model time step. To be used in the model, the wind profile must be resampled to the model resolution. The energy profile is obtained by averaging the values during an hour. Notice that the value at an hour shift is considered to be part of the hour starting at that time. To obtain the power profile, we can fit a piecewise linear curve that minimizes the distance to the continuous values, which would give the power profile shown in Fig. 2.

An inspection intuitively shows that the continuous wind profile is better approximated by the piecewise linear power profile than the energy staircase profile. However, this can also be seen by computing the ramp rates. For the energy profile, let the ramp rate for an hour be given by

$$\text{ramp}_t = e_t - e_{t-1}, \tag{1}$$

where e_t is the energy produced during time step t , and for the power profile by

$$\text{ramp}_t = p_{t+1} - p_t, \tag{2}$$

where p_t is the power output at the beginning of time step t . Table 1 shows the ramp rates of the energy and power profile for the time steps 1–3, and compares the minimum and maximum ramp rates during the period to the minimum and maximum instantaneous ramp rates of the continuous profile. Although both the energy and power profiles underestimate the maximum ramp rates due to the

Table 1
Ramp rates of wind power profile in Fig. 2

hour	ramp rate		
	energy [MWh/h]	power [MW/h]	continuous [MW/h]
1	150	400	–
2	100	–400	–
3	–250	0	–
min	–250	–400	–800
max	150	400	600

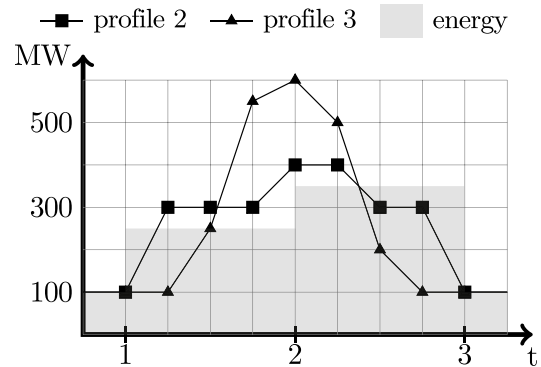


Fig. 3. Continuous wind profiles with the same energy content as in Fig. 2.

lower resolution, the power-based profile give ramp rates closer to the actual values. Also, the power profile captures the minimum and maximum output of the wind power better than the energy profile.

Another problem with the energy-based formulation is that there is not a unique energy profile for a given continuous profile. Fig. 3 shows two additional distinct continuous high resolution wind profiles that have the same energy content as in Fig. 2. Although the continuous profiles have distinctly different ramp rates and maximum values, the low resolution energy profiles will be identical. On the other hand, fitting low resolution piecewise linear power profiles will result in different profiles that better capture the variability of the continuous profile.

To show the benefits of the power-based formulation for a more realistic example, Fig. 4 shows a wind power profile from the model in Ref. [10] for 6 days. The original high resolution profile is shown as well as the fitted 4-h energy and power profiles. It can be seen that the mean absolute error (MAE) for the power profile is less than half of the MAE for the energy profile. To better quantify the agreement between the fitted profiles and the high resolution profile, we can look at the profiles for a single day, and then compute the min and max values and min and max ramp rates during that day. Table 2 shows the difference between these values for the energy and power profile compared to the high resolution profile. It can be seen that the energy profile consistently overestimates the minimum daily production and underestimates the maximum daily production. Similarly, the maximum 4 h ramp rates are also underestimated by the energy profile. The power profile performs much better at estimating both the daily min and max values and the maximum ramp rates, decreasing the average errors by an order of magnitude.

Using a piecewise linear power profile will also improve the modelling of other continuous quantities, such as demand and solar production. Thus there are two main benefits of using a power-based dispatch model as opposed to a traditional energy-based formulation. The first is the improved modelling of supply of flexibility, by correctly modelling unit ramp rates and avoiding

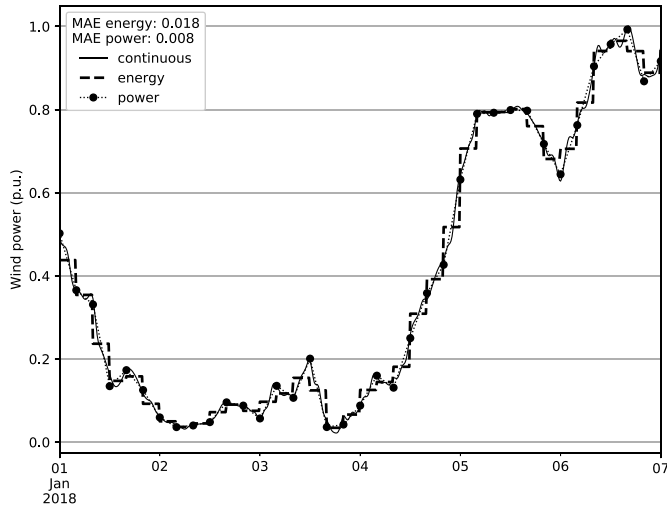


Fig. 4. Fitted power and energy profile with 4 h resolution for wind production in SE1 during 6 days.

infeasible energy schedules, and the second is an improved representation of demand of flexibility, by more accurate modelling of the variability of model inputs such as demand and VRE production. The energy-based formulation, on the other hand, overestimates the supply of flexibility and underestimates the demand of flexibility, which is a drawback when modelling future energy systems with high VRE penetration.

However, using a piecewise linear trajectory to describe the power profiles of units also has disadvantages. The main drawback is that it underestimates the flexibility of fast ramping units, as discussed in Ref. [26]. Since the maximum ramp of a unit must be within its capacity operating range, the maximum ramp rate that can be modelled is given by $(\bar{P}_g - \underline{P}_g)/\Delta$, where Δ is the time step in the model. So for units with a higher ramp rate than this, the ramp capability will be underestimated. Also, the larger the time step, the greater will be the inflexibility imposed on fast-ramping units. This is another reason why the power-based formulation can be expected to perform better for systems where ramp rates are a limiting factor, compared to systems with lots ramping flexibility. Thus the power-based formulation, unlike the energy-based formulation, can underestimate the supply of flexibility. Still, for power system security it is better to underestimate the flexibility than to overestimate it.

3. Model formulation

This section starts by giving a short overview of the original Nordic dispatch model in Section 3.1, and then presents the energy-based version of the model in Section 3.2, and the power-based

version in Section 3.3. To distinguish between quantities in energy and power, all variables and parameters that can appear in both energy and power are marked by the superscript e/p, e.g., p_{gt}^e and p_{gt}^p for production in energy and power, respectively. Quantities without a superscript are always in energy. The input parameters were computed differently depending on if they are in energy or power, as described in Section 3.4. Section 3.5 describes how unit ramps were penalized to remove unrealistic power oscillations from the power-based model.

3.1. Nordic dispatch model

The Nordic dispatch model [10] is an hourly, area-based dispatch model for the Nordic power system, modelling the generation in the different price areas in Sweden, Norway, Denmark, and Finland. The model includes 12 price areas and six different generation technologies (thermal, nuclear, reservoir hydro, run of river hydro, wind power, and solar power). There is a significant amount of reservoir hydro power production with seasonal storage, with a total reservoir capacity of 120 TWh and hydro production corresponding to roughly 55% of annual electricity generation.

The main inputs to the model are the fitted quadratic cost functions, generation capacity, hydro reservoir inflow, potential wind and solar generation, transmission capacities between different price areas, and demand profiles. The model optimizes the production in the different price areas and the content in the hydro reservoirs to meet the demand, which is modelled as an inflexible demand that can be curtailed at the maximum Nordpool price of 3000 EUR/MWh. Direct outputs of the model are production of the different types in each price area, transfers between the areas, reservoir contents, and prices which are obtained from the dual variables of the demand balance constraints. For this paper, exchanges to external price areas are fixed, meaning that the Nordic countries are modelled as an isolated system, and transmission losses between areas are set to zero. However, Section 5 shows sensitivity analysis of the results when the model was run with 1% losses. For more details regarding the model and detailed input data, see Ref. [10].

For the purpose of serving as a benchmark, the original hourly model was converted into a 15-min time resolution model, by interpolating the original hourly time series to 15-min values, as described in Section 3.4. In this paper we provide the full mathematical formulations for the low resolution energy-based and power-based versions of the model. For the formulation of the original and 15-min model, which are the same except for the time resolution, we refer to Ref. [10].

3.2. Energy-based formulation

The energy-based model formulation is to minimize the system energy costs (3) subject to demand balance (4), hydro constraints

Table 2
Daily errors for energy and power profiles compared to continuous profile from Fig. 4

	min		max		4 h ramp down		4 h ramp up	
	energy	power	energy	power	energy	power	energy	power
2018-01-01	0.027	-0.002	-0.054	0.011	0.065	-0.014	-0.000	0.027
2018-01-02	0.005	0.005	-0.004	0.002	0.020	0.004	-0.016	0.004
2018-01-03	0.013	0.014	-0.043	0.003	0.052	-0.023	-0.027	0.008
2018-01-04	0.036	-0.002	-0.118	-0.017	0.024	-0.024	-0.016	-0.001
2018-01-05	0.051	0.002	-0.007	-0.009	0.013	0.012	-0.059	0.012
2018-01-06	0.078	0.017	-0.036	-0.009	0.064	-0.009	-0.015	0.003
avg	0.035	0.006	-0.043	-0.003	0.040	-0.009	-0.022	0.009

(5)–(8), ramp rates (10)–(12), and variable limits (13)–(20). Notice that in this formulation all quantities that appear are in terms energy, i.e., constant values during the model time step. To get the correct costs, the objective is multiplied with the size of the time step, Δ . Also, the time step multiplies the inflow and withdrawal from the hydro reservoirs in (5), and the allowed ramp rates in (10)–(12).

Objective:

$$\Delta \cdot \sum_{t \in \mathcal{T}} \left(\sum_{g \in \mathcal{G}} C_{gt} (p_{gt}^e) + \sum_{a \in \mathcal{A}} VOLL \cdot d_{at}^e + \sum_{a \in \mathcal{A}} C^W \cdot w_{at}^e \right), \quad (3)$$

Demand balance:

$$\sum_{g \in \mathcal{G}_a} p_{gt}^e + res_{at}^e + ror_{at}^e + w_{at}^e + pv_{at}^e - (\bar{D}_{at}^e - d_{at}^e) - \sum_{c \in \{c^l: a_1=a\}} x_{ct}^e + \sum_{c \in \{c^l: a_2=a\}} (1-\eta) \cdot x_{ct}^e - \sum_{c \in \mathcal{C}^{Ea}} Z_{ct}^e = 0, \quad \forall a \in \mathcal{A}, t \in \mathcal{T}. \quad (4)$$

Hydro constraints:

$$r_{a,t+1} = r_{at} + \Delta (I_{at} - res_{at}^e - \overline{ROR}_{at}^e - s_{at}) \quad \forall a \in \mathcal{A}^H, t \in \mathcal{T} \quad (5)$$

$$\underline{H}_a \leq res_{at}^e + ror_{at}^e \leq \bar{H}_a \quad \forall a \in \mathcal{A}^H, t \in \mathcal{T} \quad (6)$$

$$0 \leq ror_{at}^e \leq \overline{ROR}_{at}^e \quad \forall a \in \mathcal{A}^H, t \quad (7)$$

$$r_{a,1} = R_a^{\text{ini}} \quad \forall a \in \mathcal{A}^H \quad (8)$$

$$r_{a,T+1} = R_a^{\text{end}} \quad \forall a \in \mathcal{A}^H \quad (9)$$

Ramp constraints:

$$\Delta RD_g \leq p_{g,t+1}^e - p_{gt}^e \leq \Delta RU_g \quad \forall g \in \mathcal{G}, t = 1, \dots, T-1 \quad (10)$$

$$\Delta RD_a^H \leq res_{a,t+1}^e + ror_{a,t+1}^e - res_{at}^e - ror_{at}^e \leq \Delta RU_a^H \quad \forall a \in \mathcal{A}^H, t = 1, \dots, T-1 \quad (11)$$

$$\Delta RD^{DC} \leq x_{c,t+1}^e - x_{ct}^e \leq \Delta RU^{DC} \quad \forall c \in \mathcal{C}^{DC}, t = 1, \dots, T-1 \quad (12)$$

Variable limits:

$$0 \leq d_{at}^e \leq \bar{D}_{at}^e \quad \forall a \in \mathcal{A}, t \in \mathcal{T} \quad (13)$$

$$\underline{P}_g \leq p_{gt}^e \leq \bar{P}_g \quad \forall g \in \mathcal{G}, t \in \mathcal{T} \quad (14)$$

$$0 \leq w_{at}^e \leq \bar{W}_{at}^e \quad \forall a \in \mathcal{A}, t \in \mathcal{T} \quad (15)$$

$$0 \leq pv_{at}^e \leq \bar{PV}_{at}^e \quad \forall a \in \mathcal{A}, t \in \mathcal{T} \quad (16)$$

$$0 \leq r_{at} \leq \bar{R}_a \quad \forall a \in \mathcal{A}^H, t = 2, \dots, T \quad (17)$$

$$0 \leq res_{at}^e \quad \forall a \in \mathcal{A}^H, t \in \mathcal{T} \quad (18)$$

$$0 \leq s_{at} \quad \forall a \in \mathcal{A}^H, t \in \mathcal{T} \quad (19)$$

$$0 \leq x_{ct}^e \leq \bar{X}_{ct}^e \quad \forall c \in \mathcal{C}^l, t \in \mathcal{T} \quad (20)$$

3.3. Power-based formulation

With the power-based formulation, the production trajectories are described as piecewise linear power trajectories, as illustrated in Fig. 1. However, the objective is still given as the energy cost,

$$\Delta \cdot \sum_{t \in \mathcal{T}} \left(\sum_{g \in \mathcal{G}} C_{gt} (p_{gt}^e) + \sum_{a \in \mathcal{A}} VOLL \cdot d_{at}^e + \sum_{a \in \mathcal{A}} C^W \cdot w_{at}^e \right) \quad (21)$$

where the energy-based quantities appearing are computed as the averages of the power-based variables, e.g.,

$$p_{gt}^e = \frac{p_{g,t+1}^p + p_{gt}^p}{2}$$

for p_{gt}^e , and similarly for the remaining variables. Notice that in the power-based formulation, all variables appearing in terms of energy are computed by obtaining their energy content in this way.

The demand balance is now specified as an instantaneous power balance, meaning that all variables and parameters appearing in the demand balance are power quantities:

$$\sum_{g \in \mathcal{G}_a} p_{gt}^p + res_{at}^p + ror_{at}^p + w_{at}^p + pv_{at}^p - (\bar{D}_{at}^p - d_{at}^p) - \sum_{c \in \{c^l: a_1=a\}} x_{ct}^p + \sum_{c \in \{c^l: a_2=a\}} (1-\eta) \cdot x_{ct}^p - \sum_{c \in \mathcal{C}_a^E} Z_{ct}^p = 0, \quad \forall a \in \mathcal{A}, t \in \mathcal{I}. \quad (22)$$

Since demand balance is enforced both at the beginning and end of each time step, and all variables in (22) are changing linearly within the time step, this ensures demand balance is enforced continuously during the whole planning period. Notice that demand balance is also enforced for $t = T + 1$, i.e., at the end of the last time step.

Since the hydro reservoirs are a form of energy storage, the reservoir balance (23) is still specified hourly in terms of energy. However, the variables for reservoir and run-of-river hydro production, res_{at}^p and ror_{at}^p , appear in the demand balance and must be defined in terms of power. Also the production limits (24)–(25) are enforced in terms of power. For the reservoir balance (23), the corresponding energy quantities must be used instead of the power-based values. On the other hand, the spillage s_{at} appears only in the hydro balance and can thus be kept in terms of energy. The initial and final reservoir levels (26)–(27) are enforced in the same way as for the energy-based model.

$$r_{a,t+1} = r_{at} + \Delta \left(I_{at} - res_{at}^e - 0.5 \cdot (\overline{ROR}_{a,t+1}^p + \overline{ROR}_{at}^p) - s_{at} \right) \quad \forall a \in \mathcal{A}^H, t \in \mathcal{T} \quad (23)$$

$$\underline{H}_a \leq res_{at}^p + ror_{at}^p \leq \bar{H}_a \quad \forall a \in \mathcal{A}^H, t \in \mathcal{T} \quad (24)$$

$$0 \leq ror_{at}^p \leq \overline{ROR}_{at}^p \quad \forall a \in \mathcal{A}^H, t \quad (25)$$

$$r_{a,1} = R_a^{\text{ini}} \quad \forall a \in \mathcal{A}^H \quad (26)$$

$$r_{a,T+1} = R_a^{\text{end}} \quad \forall a \in \mathcal{A}^H \quad (27)$$

The ramp constraints are the same as for the energy-based formulation except that they are enforced using the power-based quantities

$$\Delta RD_g \leq p_{g,t+1}^p - p_{gt}^p \leq \Delta RU_g \quad \forall g \in \mathcal{G}, t \in \mathcal{T} \quad (28)$$

$$\begin{aligned} \Delta RD_a^H &\leq res_{a,t+1}^p + ror_{a,t+1}^p - res_{at}^p - ror_{at}^p \\ &\leq \Delta RU_a^H \quad \forall a \in \mathcal{A}^H, t \in \mathcal{T} \end{aligned} \quad (29)$$

$$\Delta RD^{\text{DC}} \leq x_{c,t+1}^p - x_{ct}^p \leq \Delta RU^{\text{DC}} \quad \forall c \in \mathcal{C}^{\text{DC}}, t \in \mathcal{T} \quad (30)$$

and the variable limits are also the same as before, except that the time varying parameters restricting the variables in power are also given in terms of power:

$$0 \leq d_{at}^p \leq \bar{D}_{at}^p \quad \forall a \in \mathcal{A}, t \in \mathcal{I} \quad (31)$$

$$P_g \leq p_{gt}^p \leq \bar{P}_g \quad \forall g \in \mathcal{G}, t \in \mathcal{I} \quad (32)$$

$$0 \leq pv_{at}^p \leq \bar{PV}_{at}^p \quad \forall a \in \mathcal{A}, t \in \mathcal{I} \quad (33)$$

$$0 \leq r_{at} \leq \bar{R}_a \quad \forall a \in \mathcal{A}^H, t = 2, \dots, T \quad (34)$$

$$0 \leq res_{at}^p \quad \forall a \in \mathcal{A}^H, t \in \mathcal{I} \quad (35)$$

$$0 \leq s_{at} \quad \forall a \in \mathcal{A}^H, t \in \mathcal{I} \quad (36)$$

$$0 \leq w_{at}^p \leq \bar{W}_{at}^p \quad \forall a \in \mathcal{A}, t \in \mathcal{I} \quad (37)$$

$$0 \leq x_{ct}^p \leq \bar{X}_{ct}^p \quad \forall c \in \mathcal{C}^I, t \in \mathcal{I} \quad (38)$$

3.4. Constructing the input time series

The energy-based and power-based versions of the model were compared to a benchmark model with 15-min time resolution. The 15-min time series for the high-resolution model were obtained by interpolating the original hourly time series, using the methods shown in Table 3. In general, a standard way to create smooth high resolution profiles is to use cubic splines, which was used for demand, wind, and solar production. For transfers to external areas and hydro inflows, which have less intra-hour variability, linear interpolation was used. The time series for exchange capacities were not interpolated, since these are effectively constant during an hour. In Section 5, we also performed sensitivity analysis regarding the choice of interpolation methods used to create the 15-min time series.

The 15-min model was used as a benchmark with which to compare the low resolution models. To make a fair comparison between the energy-based and power-based formulations, all low-resolution time series were obtained from the 15-min time series in the following manner. For the energy-based model, the time series were obtained by averaging the 15-min values over a Δ -hour period. For the power-based model, piecewise linear profiles were fitted that minimized the deviation from the 15-min profiles.

Fig. 5 illustrates the fitting of the piecewise linear power profile. Notice that the high resolution data points are treated as

instantaneous power values when fitting the low resolution power profiles. Let (x_i, y_i) for $i = 1, \dots, N$ be the set of equally spaced high resolution (15-min) data points, and $f_j(x) = a_jx + b_j$ for $j = 1, \dots, n$ be the set of linear segments to be fitted. It holds that $N = \Delta \cdot n + 1$ where Δ is the number of data points per segment (if, e.g., the resolution $\Delta = 2$ h this means that there are $\Delta = 4 \cdot 2 = 8$ points per segment, since the data has 15-min time resolution). Each data point can be mapped to the corresponding segment by

$$j(i) = \left\lfloor \frac{i-1}{\Delta} \right\rfloor + 1, \quad (39)$$

meaning that the first Δ points are mapped to the first segment. The last data point (x_N, y_N) is mapped to the segment n , which thus has $\Delta + 1$ data points. The knot points, at which the y-values of the piecewise linear power profile will be defined, are given by $\hat{x}_j = x_{(j-1)\Delta+1}$ for $j = 1, \dots, n + 1$. The last segment n has two knot points. Fitting the power profile considering the root mean squared error (RMSE) can then be formulated as the following quadratic optimization problem:

$$\min \sum_{i=1}^N (\epsilon_i^+)^2 + (\epsilon_i^-)^2 \quad \text{such that} \quad (40)$$

$$\epsilon_i^+ - \epsilon_i^- = f_{j(i)}(x_i) - y_i \quad \forall i = 1, \dots, N \quad (41)$$

$$f_j(\hat{x}_{j+1}) = f_{j+1}(\hat{x}_{j+1}) \quad \forall j = 1, \dots, n - 1 \quad (42)$$

$$y_j \leq f_j(\hat{x}_j) \leq \bar{y}_j \quad \forall j = 1, \dots, n \quad (43)$$

$$y_{n+1} \leq f_n(\hat{x}_{n+1}) \leq \bar{y}_{n+1} \quad (44)$$

$$\epsilon_i^+, \epsilon_i^- \geq 0 \quad \forall i = 1, \dots, N \quad (45)$$

Table 3
Interpolation of 15-min data.

Parameter	Method
Demand (D)	cubic spline
Solar power (PV)	cubic spline
Run of river (ROR)	linear
Wind power (W)	cubic spline
Exchange capacity (X)	constant
External transfer (Z)	linear
Reservoir inflow (I)	linear

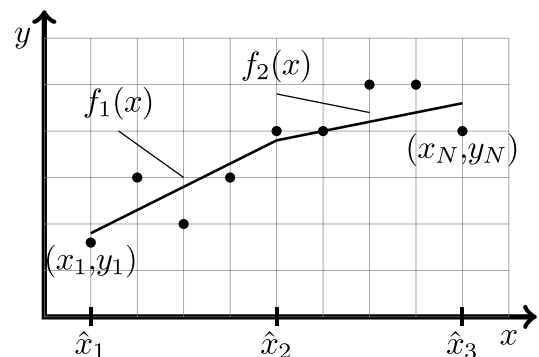


Fig. 5. Fitting piecewise linear power profile with $n = 2$ segments.

The optimization variables are the fitting errors ϵ_i^+ , ϵ_i^- for $i = 1, \dots, N$ and the coefficients of the linear segments, a_j, b_j for $j = 1, \dots, n$. Eq. (41) forces ϵ_i^+ and ϵ_i^- to take on the positive and negative error, respectively, for each data point and (42) ensures continuity of the linear segments. The bounds on the piecewise linear profile at the knot points are enforced by (43)–(44), where $\underline{y}_j, \bar{y}_j$ for $j = 1, \dots, n + 1$ are the lower/upper bounds, and (45) enforces positivity of the fitting errors. It is also possible to enforce that the total energy content of the fitted profile is the same as the high-resolution profile, by adding (46) to the constraints:

$$\sum_{j=2}^n f_j(\hat{x}_j) + \frac{f_1(\hat{x}_1) + f_n(\hat{x}_{n+1})}{2} = \left(\sum_{i=2}^{N-1} y_i + \frac{y_1 + y_N}{2} \right) / \Delta \quad (46)$$

Fig. 6 shows the power profile fit for solar production in Sweden over 7 days. Notice that if the bounds for the power profile are constant in (43), the peaks of the power profile will not match the peaks in the 15-min data. However, introducing time-varying bounds calculated locally from the 15-min data the peak values could be made to match the data, as shown by fit 2 in Fig. 6.

3.5. Penalizing power oscillations

Unlike for most energy system models [28–31], the objective in the Nordic dispatch model is quadratic. This was important for the performance of the model, as using quadratic costs significantly increased the accuracy of the model when compared to historical data [10]. Also, linear models can produce excessive cycling of units that require ramp penalizations to be reduced [29]. However, the objective is quadratic in terms of energy, and not in terms of power. Thus what matters for the cost is only the average energy produced by different generation types each time step. Hence, it is possible to obtain solutions to the power-based model where the power production oscillates as shown in Fig. 7. What happens is that the thermal production in different areas oscillate in counter-phase, to even out the fluctuations in the total production. Since only the average energy during a time step enters the objective, these oscillations do not impose any additional costs in the model. In other words, there are multiple vertices, or power trajectories, giving the same global optimum. In order to remove such unrealistic oscillations, we introduced a small penalization for ramps in the power-based model. This was done by adding

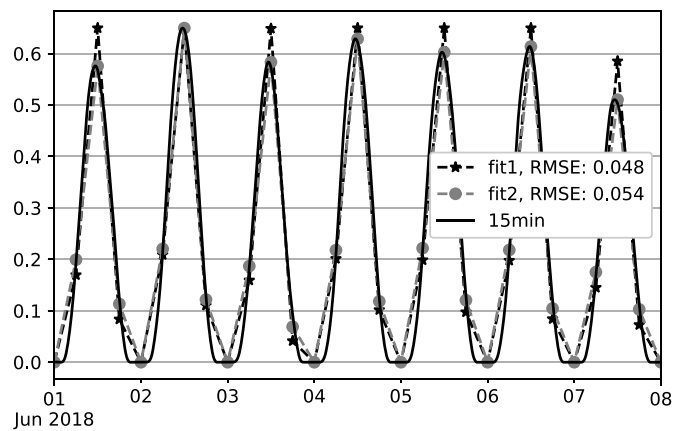


Fig. 6. Fitting 6 h resolution power profile for solar power in Sweden by minimizing the RMSE. Fit 1 has a constant upper limit for the power profile, while fit 2 has variable upper limits, computed as the maximum 15-min value over a 24-h rolling window.

$$p_{g,t+1}^p - p_{gt}^p = \delta_{gt}^+ - \delta_{gt}^- \quad \forall g \in \mathcal{G}^T, t \quad (47)$$

$$\delta_{gt}^+, \delta_{gt}^- \geq 0 \quad \forall g \in \mathcal{G}^T, t \quad (48)$$

to the model and introducing a penalization term in the objective, thus replacing (21) by:

$$\Delta \cdot \sum_{t \in T} \left(\sum_{g \in \mathcal{G}} C_{gt} \cdot p_{gt}^e + \sum_{a \in A} VOLL \cdot d_{at}^e + \sum_{a \in A} C^w \cdot w_{at}^e \right) + \mu \sum_{g \in \mathcal{G}^T} \sum_{t \in T} (\delta_{gt}^+ + \delta_{gt}^-) \quad (49)$$

As shown in Fig. 7, this eliminated the power oscillations. A value of $\mu = 4.5 \cdot 10^{-4}$ was found to be sufficient and was used in the power-based model. Note that the penalization for the ramp oscillations was removed when comparing the objective values of the energy-based and power-based formulations in Section 4 and Section 5.

4. Results

The models were implemented in Python and solved using Gurobi 9.0.2 on a PC with Intel Core i7-4790 CPU @ 3.6 GHz and 32 GB of RAM. The power and energy-based models were implemented with time steps of 1–4 and 6 h, and compared to the benchmark 15-min time resolution model. The method used to construct the time series with different time resolutions is described in Section 3.4.

The models were solved for 2018 for two different cases, one with increased renewable production which created the need for curtailing wind power, and one case with decreased nuclear production which created the need for load shedding. The original generation mix in the Nordic power system for 2018 was 55% hydro power production, 23% nuclear production, 12% thermal generation, and 10% wind power. There were 12 price areas and 8736 h in the simulated time period, and the benchmark model had 4.2 million variables, 3.3 million constraints, and 12.1 million non-zeros. Note that the year 2018 was chosen since this was the most recent year with hydro power inflow data available in the original model [10], but Section 5 also shows the results when the case studies were run for 2017, to show the impact of a different year. In the following subsections we compare the performance of the models for the two case studies in greater detail.

4.1. Wind curtailment

To get a case with wind power curtailment, the wind power production in Sweden was increased by 100% compared to the historical values for 2018 and the PV solar power in Sweden was increased to 5 GW. Fig. 8 shows the total amount of wind power curtailment in the models run with different time resolution. Notice that the energy-based model consistently underestimated the curtailment, the difference compared to the benchmark model increasing as the model time step increases, giving deviations up to 90%. On the other hand, the power-based formulation gave an estimate of the curtailment closer to the benchmark model, being off by at most 19%. Fig. 9 shows the time series and duration curves for the total wind power curtailment, for the 6 h models. The duration curves show that the result for the power-based model was closer to the 15-min benchmark model compared to the energy-based model, both in terms of estimating the maximum amount of curtailment and the number of hours with curtailment, which was around 200.

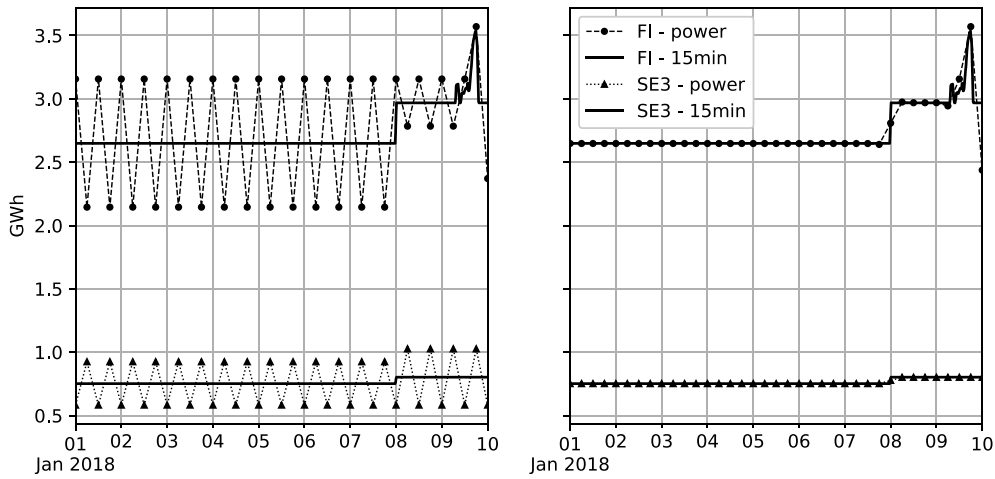


Fig. 7. Thermal production in Finland (FI) and Sweden (SE3) for power-based model with 6 h time step and 15-min benchmark model, without ramp penalization (left) and with ramp penalization (right) with $\mu = 4.5 \cdot 10^{-4}$. The legend is the same for both graphs. Notice that the power oscillations in FI and SE3 are in counter-phase.

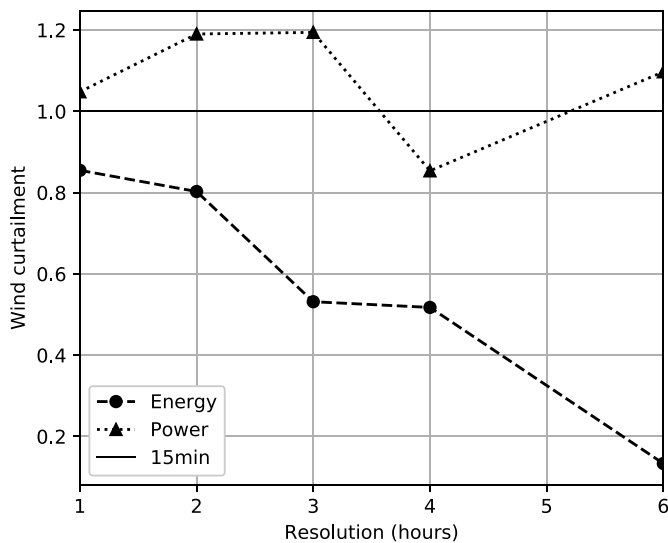


Fig. 8. Total yearly wind curtailment in the Nordic system for different model time resolutions. Values are normalized with results for the benchmark model, which is 35.8 GWh.

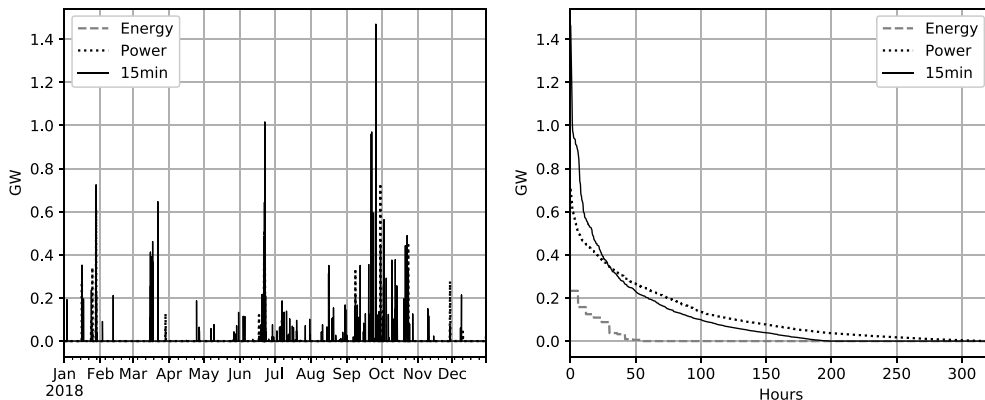


Fig. 9. Total yearly wind curtailment in the Nordic system for models with 6 h time resolution, plotted as time series (left) and duration curves (right).

Fig. 10 shows the objective values obtained when solving the models with different time resolution. Both models underestimated the system cost, but the difference for the energy-based model was much larger, 1.6% for 6 h resolution compared to 0.4% for the power-based model. The decreased costs for the energy-based model can not only be explained by decreased wind curtailment compared to the benchmark model. Assuming that the average thermal cost to replace curtailed wind power is 30 EUR/MWh, the potential cost decrease of avoiding the 36 GWh curtailment in the benchmark model is $3 \cdot 10^4 \text{ EUR/GWh} \cdot 36 \text{ GWh} = 1.08 \cdot 10^6 \text{ EUR}$, which is only 0.1% of the total costs ($8.75 \cdot 10^8 \text{ EUR}$). In general, decreasing the time resolution can be expected to decrease the costs, since the variability of the inputs such as demand and VRE production is reduced, allowing smoother production profiles for the thermal generation, which decreases the costs due to the quadratic cost functions.

The time it took to solve the models is shown in Fig. 11. Notice that the time needed to build the optimization problem (which was done using Gurobi's Python api) and the time spent in the solver are shown separately, but together comprise the total solution time. For both the energy-based and power-based models, the solution time decreased by about a factor 9 when going from 1 h time resolution to 6 h resolution. Notice that the solution time for the power-based model was consistently somewhat higher than for the energy-based model, which is different from the results obtained in Ref. [25]. The reason that the power-based formulation was harder

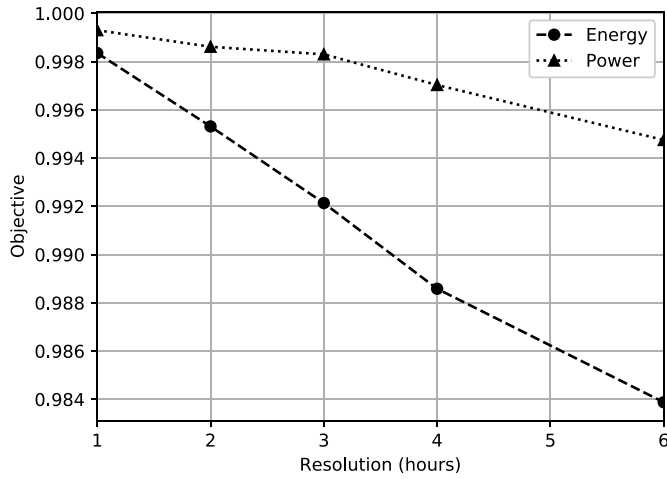


Fig. 10. Objective value for different model resolutions. Values are normalized with results for the benchmark model, which is $8.75 \cdot 10^8$ EUR. For the power-based model the cost for ramp penalizations has been excluded.

to solve can be due to the additional complexity introduced by the constraints penalizing the power oscillations, as described in Section 3.5.

4.2. Load shedding

To get a case with load shedding, 3 out of 4 reactors (block 1–3) at the nuclear power plant Ringhals in SE3 were removed, and VRE production in Sweden was set to the actual values for 2018. Fig. 12 shows the total load shedding for the models with different time steps. Similarly to the case with curtailment, the energy-based model consistently underestimated the amount of load shedding. On the other hand, the power-based model overestimated the load shedding, but gave results closer to the benchmark model for resolutions of 2–6 h, with a maximum error of 26% compared to 34% for the energy-based model. Fig. 13 shows the load shedding for the 6 h models, plotted as time series and duration curves. Notice that although the 6 h power-based model overestimated the total amount of load shedding, the peak load shedding in GW was quite close to the benchmark model.

Fig. 14 shows the objective values obtained for the low resolution models. In this case, the direct influence of the load shedding on the costs was much stronger compared to the previous case with

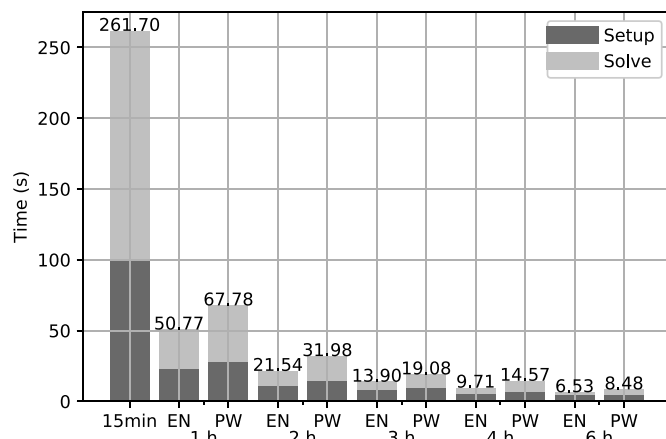


Fig. 11. Model solution duration for different time resolutions.

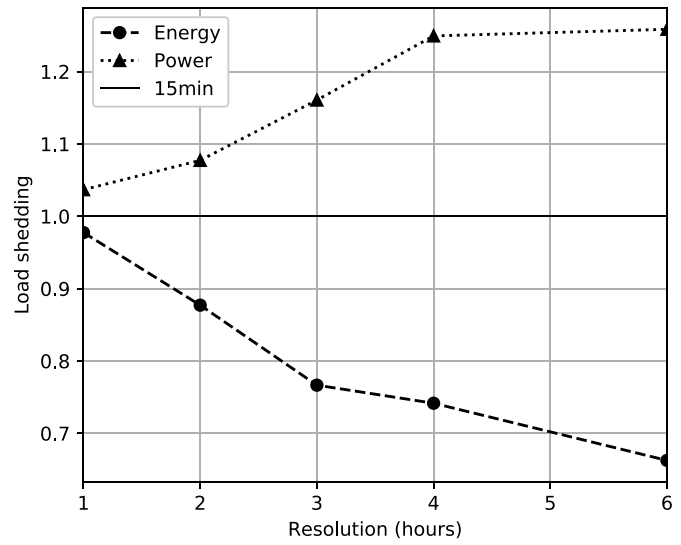


Fig. 12. Total yearly load shedding in the Nordic system for different model time resolutions. Values are normalized with results for the benchmark model, which is 85.3 GWh.

renewable curtailment. For the power-based model with 6 h time resolution, the additional load shedding compared to the benchmark model was 22 GWh, which, given the load shedding cost of 3000 EUR/MWh, amounts to 66 million EUR, or 2% of the total costs for the benchmark model. Thus the increased costs for the power-based model resulted mostly from the increased load shedding. On the other hand, the energy-based model underestimated the amount of load shedding and thus also the costs.

Fig. 15 shows the time needed to run the models, which was similar to the previous case study with curtailment.

5. Sensitivity analysis

This section presents sensitivity analysis performed to investigate the robustness of the results from Section 4. One important factor which could influence the results was the method used to interpolate the time series for the high resolution model. As shown in Table 3, the high resolution time series were obtained using linear or spline interpolations of the hourly data. To investigate the effects of the choice of interpolation methods, the case studies from Section 4 were rerun when all time series data were interpolated with either linear or spline interpolation (except the exchange capacities which were fixed during an hour). Figs. 16 and 17 show the objective function value for the curtailment and loadshed case study, respectively, using both spline and linear interpolations.

The case studies in Section 4 were also run for 2017 instead of 2018, and applying a 1% loss to internal transfers, to check the robustness of the results with respect to the modelled year and losses. The results are also shown in Figs. 16 and 17.

Fig. 16 shows that the results for the curtailment case study were quite similar across the different settings. Using the power-based model gave results close to the high resolution model for all resolutions, while the energy-based model underestimated curtailment and therefore also the operation cost. For the loadshed case study, shown in Fig. 17, the results were also similar for the different settings. Using the power-based formulation overestimated loadshed and cost, while using the energy-based formulation underestimated them. However, in this case the energy-based formulation gave total costs closer to the result from the 15-min model for some settings. In particular, the energy-based

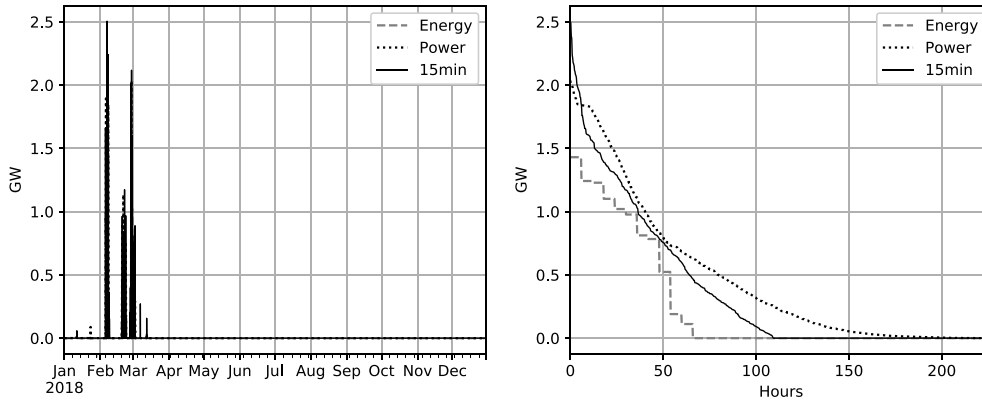


Fig. 13. Total yearly load shedding in the Nordic system for models with 6 h time resolution, plotted as time series (left) and duration curves (right).

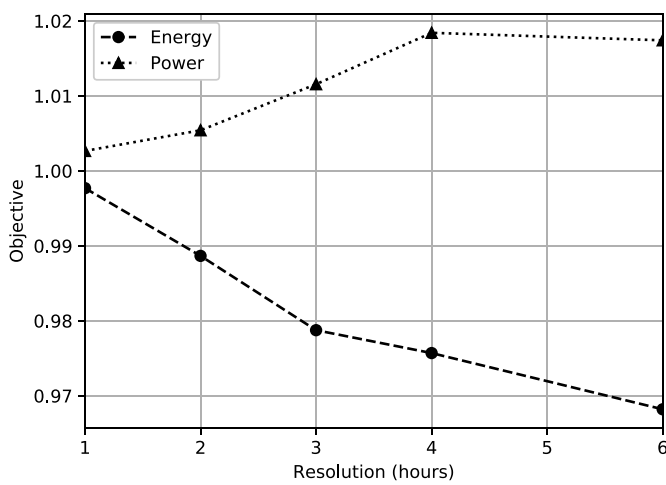


Fig. 14. Objective value for different model resolutions. Values are normalized with results for the benchmark model, which is $2.97 \cdot 10^9$ EUR. For the power-based model the cost for ramp penalizations has been excluded.

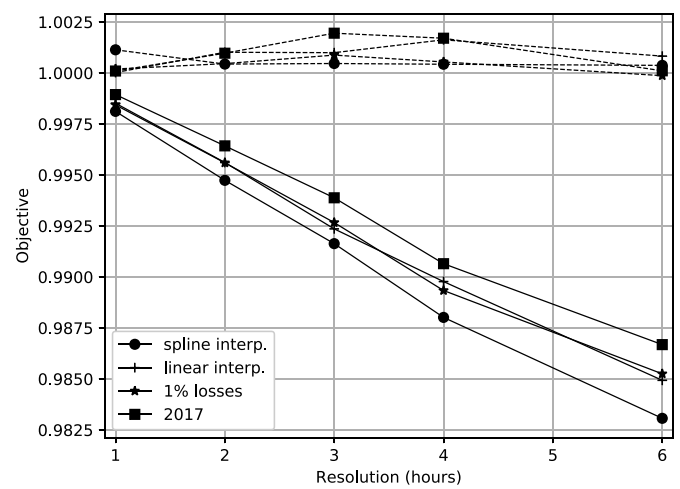


Fig. 16. Sensitivity analysis of the results for the curtailment case study. The objectives are normalized relative to the results from the high resolution model, which is different for each case. Dashed lines show results for power-based model and solid lines for energy-based model.

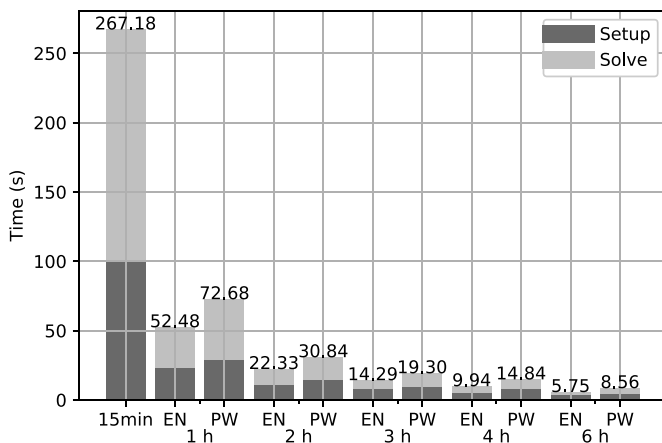


Fig. 15. Model solution duration for different time resolutions.

formulation performed better than the power-based model for 2017, and when using linear interpolation for the time series. This shows that the power-based formulation is not guaranteed to give better results than the energy-based formulation. As discussed in Section 2, the power-based formulation underestimates the flexibility of units with high ramp rates, especially as the time

resolution of the model increases. This applies to the studied system, since it includes large amounts of hydro power which has high flexibility. However, it should also be noted that using a linear interpolation to calculate the 15-min values underestimates the intra-hour variability, which can explain why the energy-based formulation performed better in this case. Also, even if energy-based models provide good results in terms of costs, the solutions are not guaranteed to be feasible, since it does not guarantee the existence of a feasible power trajectory, overestimating the flexibility of dispatchable units and underestimating the variability of demand and VRE production.

6. Conclusion

In this paper we proposed a power-based version of a dispatch model using clustered time periods to reduce the size and complexity of the model. Compared to the conventional energy-based model, the power-based model allows to lower the time resolution while better preserving the properties of the time series inputs used in the model, such as ramp rates and peak values. This increases the accuracy of the power-based model compared to the energy-based model when increasing the size of the time steps, and is particularly useful when simulating systems with high renewable penetration, since it is paramount to accurately represent

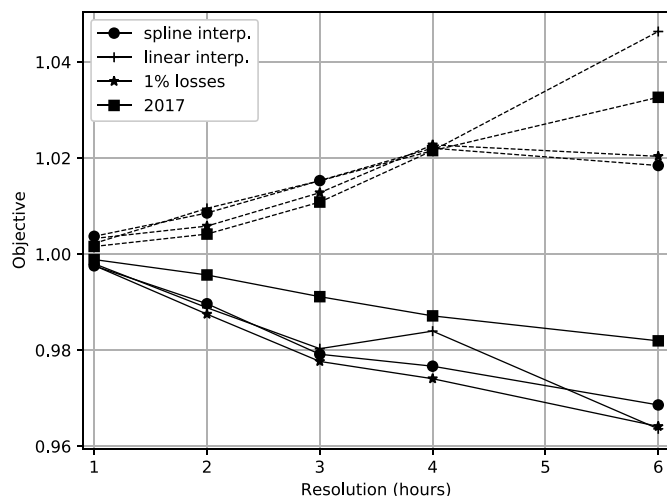


Fig. 17. Sensitivity analysis of the results for the loadshed case study. The objectives are normalized relative to the results from the high resolution model, which is different for each case. Dashed lines show results for power-based model and solid lines for energy-based model.

renewable variability.

We evaluated the energy-based and power-based models for different time resolutions using two case studies, one with increased renewable generation and curtailment, and one with decreased conventional generation and load shedding. For time steps between 2 and 6 h, the power-based model gave results closer to the 15-min benchmark model, both in terms of total energy values (energy curtailed or amount of load shedding in energy) and in terms of peak values. For example, the power-based model with 6 h time resolution gave a difference of 10% for total curtailment compared to the benchmark model, while solving 30 times faster. The power-based model also gave total costs closer to the benchmark model compared to the energy-based model for most cases. Interestingly, the power-based formulation overestimated demand curtailment while the energy-based model underestimated it. This suggests that the power-based dispatch model can be useful for applications where it is important to decrease the complexity of the model while maintaining relatively accurate modelling results, and not underestimating load curtailment. As future research, the power-based dispatch model with lower time resolution could be integrated into a model for generation expansion planning, to study if this gives improved investment decisions, compared to using an energy-based dispatch model with the same time resolution.

Funding sources

This work was supported by TNO's internal R&D projects Innovative Flexibility Options and Energy Market Modelling (project numbers 060.42856 and 060.47628), as well as by the Swedish Energy Agency through the SampspEL research program (project number 42976-1).

CRediT authorship contribution statement

Elis Nycander: Methodology, Software, Investigation, Writing – original draft. **Germán Morales-España:** Methodology, Writing – review & editing. **Lennart Söder:** Conceptualization, Writing – review & editing, Supervision.

Declaration of competing interest

The authors declare that they have no known competing financial interests or personal relationships that could have appeared to influence the work reported in this paper.

References

- [1] R. Goić, J. Krstulović, D. Jakus, Simulation of aggregate wind farm short-term production variations, *Renew. Energy* 35 (11) (2010) 2602–2609, <https://doi.org/10.1016/j.renene.2010.04.005>.
- [2] M. Shahriari, S. Blumsack, Scaling of wind energy variability over space and time, *Appl. Energy* 195 (2017) 572–585, <https://doi.org/10.1016/j.apenergy.2017.03.073>.
- [3] H. Holttinen, Hourly wind power variations in the nordic countries, *Wind Energy* 8 (2) (2005) 173–195, <https://doi.org/10.1002/we.144>.
- [4] N. Ohlendorf, W.-P. Schill, Frequency and duration of low-wind-power events in Germany, *Environ. Res. Lett.* 15 (8) (2020), 084045, <https://doi.org/10.1088/1748-9326/ab91e9>.
- [5] S. Rose, J. Apt, What can reanalysis data tell us about wind power? *Renew. Energy* 83 (2015) 963–969, <https://doi.org/10.1016/j.renene.2015.05.027>.
- [6] P. Coker, J. Barlow, T. Cockerill, D. Shipworth, Measuring significant variability characteristics: an assessment of three UK renewables, *Renew. Energy* 53 (2013) 111–120, <https://doi.org/10.1016/j.renene.2012.11.013>.
- [7] I.-C. Gonzalez-Romero, S. Wogrin, T. Gómez, Review on generation and transmission expansion co-planning models under a market environment, *IET Generation, Transm. Distrib.* 14 (6) (2020) 931–944, <https://doi.org/10.1049/iet-gtd.2019.0123>.
- [8] M. Davidson, D. Zhang, W. Xiong, X. Zhang, V. Karplus, Modelling the Potential for Wind Energy Integration on China's Coal-Heavy Electricity Grid, *Nat. Energy* 1, doi:<https://doi.org/10.1038/nenergy.2016.86>.
- [9] M. Waite, V. Modi, Modeling wind power curtailment with increased capacity in a regional electricity grid supplying a dense urban demand, *Appl. Energy* 183 (2016) 299–317, <https://doi.org/10.1016/j.apenergy.2016.08.078>.
- [10] E. Nycander, L. Söder, J. Olauson, R. Eriksson, Curtailment analysis for the nordic power system considering transmission capacity, inertia limits and generation flexibility, *Renew. Energy* 152 (2020) 942–960, <https://doi.org/10.1016/j.renene.2020.01.059>.
- [11] E.M. Garrige, J. Deane, P. Leahy, How much wind energy will be curtailed on the 2020 Irish power system? *Renew. Energy* 55 (2013) 544–553, <https://doi.org/10.1016/j.renene.2013.01.013>.
- [12] I. Graabak, M. Korpás, S. Jaehnert, M. Belsnes, Balancing future variable wind and solar power production in central-west europe with Norwegian hydropower, *Energy* 168 (2019) 870–882, <https://doi.org/10.1016/j.energy.2018.11.068>.
- [13] T. Rasku, J. Miettinen, E. Rinne, J. Kiviluoma, Impact of 15-day energy forecasts on the hydro-thermal scheduling of a future nordic power system, *Energy* 192 (2020), 116668, <https://doi.org/10.1016/j.energy.2019.116668>.
- [14] J. Lin, L. Cheng, Y. Chang, K. Zhang, B. Shu, G. Liu, Reliability based power systems planning and operation with wind power integration: a review to models, algorithms and applications, *Renew. Sustain. Energy Rev.* 31 (2014) 921–934, <https://doi.org/10.1016/j.rser.2013.12.034>.
- [15] A. Ali Kadhem, N.I. Abdul Wahab, I. Aris, J. Jasni, A.N. Abdalla, Computational techniques for assessing the reliability and sustainability of electrical power systems: a review, *Renew. Sustain. Energy Rev.* 80 (2017) 1175–1186, <https://doi.org/10.1016/j.rser.2017.05.276>.
- [16] J. Nelson, J. Johnston, A. Mileva, M. Fripp, I. Hoffman, A. Petros-Good, C. Blanco, D.M. Kammen, High-resolution modeling of the western north american power system demonstrates low-cost and low-carbon futures, *Energy Pol.* 43 (2012) 436–447, <https://doi.org/10.1016/j.enpol.2012.01.031>.
- [17] S. Wogrin, D. Tejada-Arango, S. Delikaraoglou, A. Botterud, Assessing the impact of inertia and reactive power constraints in generation expansion planning, *Appl. Energy* 280 (2020), 115925, <https://doi.org/10.1016/j.apenergy.2020.115925>.
- [18] R. Loulou, G. Goldstein, K. Noble, Documentation for the MARKAL Family of Models, Energy Technology Systems Analysis Programme, 2004. URL, https://iea-etsap.org/MrkiDoc-I_StdMARKAL.pdf.
- [19] A. Fattahi, S. Manuel, J. Sijm, G. Morales-España, A. Faaij, Measuring accuracy and computational capacity trade-offs in an hourly integrated energy system model, *Adv. Appl. Energy* 1 (2021), 100009, <https://doi.org/10.1016/j.adapen.2021.100009>.
- [20] European Network Transmission System Operators for Electricity (ENTSO-E), Mid Term Adequacy Forecast Appendix 2: methodology, 2020. URL, https://eepublicdownloads.entsoe.eu/clean-documents/sdc-documents/MAF/2020/MAF_2020_Appendix_2_Methodology.pdf.
- [21] G. Morales-España, J.M. Latorre, A. Ramos, Tight and compact mip formulation of start-up and shut-down ramping in unit commitment, *IEEE Trans. Power Syst.* 28 (2) (2013) 1288–1296, <https://doi.org/10.1109/TPWRS.2012.2222938>.
- [22] G. Morales-España, C. Gentile, A. Ramos, Tight mip formulations of the power-based unit commitment problem, *Spectrum* 37 (4) (2015) 929–950, <https://doi.org/10.1007/s00291-015-0400-4>.

- [23] G. Morales-España, R. Baldick, J. García-González, A. Ramos, Power-capacity and ramp-capability reserves for wind integration in power-based UC, *IEEE Trans. Sustain. Energy* 7 (2) (2016) 614–624, <https://doi.org/10.1109/TSTE.2015.2498399>.
- [24] E. Nycander, G. Morales-España, L. Söder, Security constrained unit commitment with continuous time-varying reserves, *Elec. Power Syst. Res.* 199 (2021), 107276, <https://doi.org/10.1016/j.epsr.2021.107276>.
- [25] R. Philipsen, G. Morales-España, M. de Weerd, L. de Vries, Trading power instead of energy in day-ahead electricity markets, *Appl. Energy* 233–234 (2019) 802–815, <https://doi.org/10.1016/j.apenergy.2018.09.205>.
- [26] G. Morales-España, L. Ramírez-Elizondo, B.F. Hobbs, Hidden power system inflexibilities imposed by traditional unit commitment formulations, *Appl. Energy* 191 (2017) 223–238, <https://doi.org/10.1016/j.apenergy.2017.01.089>.
- [27] G. Morales-España, A. Ramos, J. García-González, An mip formulation for joint market-clearing of energy and reserves based on ramp scheduling, *IEEE Trans. Power Syst.* 29 (1) (2014) 476–488, <https://doi.org/10.1109/TPWRS.2013.2259601>.
- [28] P. Sørensen, I. Norheim, P. Meibom, K. Uhlen, Simulations of wind power integration with complementary power system planning tools, *Elec. Power Syst. Res.* 78 (6) (2008) 1069–1079, <https://doi.org/10.1016/j.epsr.2007.08.008>.
- [29] J. Goop, Modelling Interactions between Distributed Energy Technologies and the Centralised Electricity Supply System, URL, Chalmers University of Technology, 2017. Ph.D. thesis, <https://publications.lib.chalmers.se/records/fulltext/251520/251520.pdf>.
- [30] F. Wiese, R. Bramstoft, H. Koduvere, A. Pizarro Alonso, O. Balyk, J.G. Kirkerud, Åsa Grytli Tveten, T.F. Bolkesjø, M. Münster, H. Ravn, Balmorel open source energy system model, *Energy Strat. Rev.* 20 (2018) 26–34, <https://doi.org/10.1016/j.esr.2018.01.003>.
- [31] L. Hirth, The European Electricity Market Model EMMA - Model Documentation, Tech. rep., Neon Neue Energiökonomi GmbH, 2017. URL, <https://neon.energy/emma-documentation.pdf>.